PRDM16 enhances nuclear receptor-dependent transcription of the brown fat-specific *Ucp1* gene through interactions with Mediator subunit MED1

Satoshi Iida,[1] Wei Chen,[1] Tomoyoshi Nakadai,[1] Yoshiaki Ohkuma,[2] and Robert G. Roeder[1]

[1]Laboratory of Biochemistry and Molecular Biology, The Rockefeller University, New York, New York 10065, USA; [2]Laboratory of Gene Regulation, Graduate School of Medicine and Pharmaceutical Science, University of Toyama, Toyama 930-0194, Japan

PR domain-containing 16 (PRDM16) induces expression of brown fat-specific genes in brown and beige adipocytes, although the underlying transcription-related mechanisms remain largely unknown. Here, in vitro studies show that PRDM16, through its zinc finger domains, directly interacts with the MED1 subunit of the Mediator complex, is recruited to the enhancer of the brown fat-specific uncoupling protein 1 (*Ucp1*) gene through this interaction, and enhances thyroid hormone receptor (TR)-driven transcription in a biochemically defined system in a Mediator-dependent manner, thus providing a direct link to the general transcription machinery. Complementary cell-based studies show that upon forskolin treatment, PRDM16 induces *Ucp1* expression in undifferentiated murine embryonic fibroblasts, that this induction depends on MED1 and TR, and, consistent with a direct effect, that PRDM16 is recruited to the *Ucp1* enhancer. Related studies have defined MED1 and PRDM16 interaction domains important for *Ucp1* versus *Ppargc1a* induction by PRDM16. These results reveal novel mechanisms for PRDM16 function through the Mediator complex.

[*Keywords*: PRDM16; Mediator/MED1; *Ucp1*; nuclear receptor; transcriptional regulation; brown/beige adipocytes]

Supplemental material is available for this article.

Received September 17, 2014; revised version accepted December 22, 2014.

Adipose tissues contain three functionally different types of fat cells: white, brown, and beige adipocytes (Rosen and Spiegelman 2006; Wu et al. 2012, 2013). White fat cells store energy in the form of triglycerides (lipids), whereas brown fat cells consume energy to produce heat (Cannon and Nedergaard 2004). Thus, in response to cold exposure and activation of the β-adrenergic signaling pathway, brown fat cells express a series of genes, such as uncoupling protein 1 (*Ucp1*), that effect thermogenesis (Cannon and Nedergaard 2004). The more recently identified beige fat cells reside in white adipose depots and rapidly respond to cyclic AMP (cAMP), which mimics β-adrenergic stimulation, to express genes (including *Ucp1*) related to respiration and energy expenditure (Wu et al. 2012, 2013). Because of their specialized functions in energy consumption, brown and beige fat cells are of great interest with respect to potential therapeutic applications to counteract diabetes and related disorders (Harms and Seale 2013).

In adipocytes, ligand-activated nuclear receptors (NRs), especially peroxisome proliferator-activated receptor γ (PPARγ) and thyroid hormone receptor (TR), play pivotal roles in transcriptional regulation pathways involved in cell differentiation and cellular function (Rosen and Spiegelman 2001; Rosen et al. 2002; Chen et al. 2009; Mishra et al. 2010). Like other transcriptional activators (Roeder 2003), NRs act in conjunction with a diverse group of interacting transcriptional cofactors that may also play key roles in cell-specific transcription. These entities include factors that act through chromatin modifications (ATP-dependent chromatin remodeling factors and histone-modifying enzymes such as p300) and others (such as the Mediator) that act more directly (Glass and Rosenfeld 2000; McKenna and O'Malley 2002; Lonard and O'Malley 2006). The Mediator, which has been broadly implicated in NR function (Chen and Roeder 2011), is a large 30-subunit coactivator complex that, by directly bridging transcription activators and components

Corresponding author: roeder@rockefeller.edu
Article is online at http://www.genesdev.org/cgi/doi/10.1101/gad.252809.114.

of general transcription machinery (RNA polymerase II [Pol II] and general initiation factors), facilitates the formation and/or function of the preinitiation complex at the core promoter (Malik and Roeder 2010). Mediator interacts strongly with the ligand-induced activation domains of NRs, including those of PPARγ and TRα, through LxxLL motifs in the MED1 subunit. The involvement of MED1/Mediator in PPARγ and TRα function has been documented both in vitro and in vivo (Fondell et al. 1996; Ge et al. 2002; Chen and Roeder 2011; Fondell 2013).

Two cell-specific transcriptional coactivators, PPARγ coactivator-1α (PGC-1α, encoded by *Ppargc1a*) and PR domain-containing 16 (PRDM16), have been shown to serve as important molecular determinants of the brown fat cell phenotype (Kajimura et al. 2010). PGC-1α was identified as a PPARγ-interacting protein that is abundant in brown adipose tissue (BAT) and enhances PPARγ- and TR-dependent expression of the brown adipocyte-specific *Ucp1* gene (Puigserver et al. 1998). Mechanistically, PGC-1α directly interacts with enhancer-bound PPARγ and TR and then, through distinct domains, directly interacts with and recruits the histone acetyltransferase p300 and (through MED1) the Mediator (Puigserver et al. 1998; Wallberg et al. 2003; Chen et al. 2009). Studies with *Ppargc1a*-null mice showed that PGC-1α is essential for expression of thermogenic genes such as *Ucp1*, albeit not for brown fat cell differentiation per se (Lin et al. 2004; Uldry et al. 2006).

PRDM16, of special interest here, was identified as a BAT-selective factor (Seale et al. 2007) that promotes differentiation of *Myf5*-positive myogenic precursor cells into brown fat cells while prohibiting myogenic differentiation (Seale et al. 2008). PRDM16 also induces robust expression of BAT-selective genes such as *Ucp1* and *Ppargc1a* when ectopically expressed in murine embryonic fibroblast (MEF) cells (Seale et al. 2007) and is involved in BAT-selective gene expression in beige fat cells (Seale et al. 2011; Cohen et al. 2014). Mechanistically, the adipogenic functions of PRDM16 do not require either the known DNA-binding activities of the two zinc finger domains (ZF1 and ZF2) or the SET domain-related N-terminal PR domain (Seale et al. 2007; Kajimura et al. 2009). However, PRDM16 has been reported to interact, apparently directly through its two zinc finger domains, with several transcription activators and cofactors that include PPARγ (Seale et al. 2008), C/EBPβ (Kajimura et al. 2009), and PGC-1α (Seale et al. 2007; Kajimura et al. 2008), and roles for ZF1 in C/EBPβ-related (Kajimura et al. 2009) and EHMT1-related (Ohno et al. 2013) adipogenic functions have been established. However, the molecular basis of the downstream transcriptional activation and repression mechanisms by PRDM16 remains poorly understood.

Here we show that PRDM16, through its ZF1 domain, interacts directly with the Mediator through its MED1 subunit and that this interaction is critical for PRDM16-dependent *Ucp1* transcription. Thus, in vitro studies show that PRDM16 can be recruited to the *Ucp1* enhancer through an interaction with either MED1 or PGC-1α and that it can enhance TRα-driven transcription in a reconstituted cell-free system in a Mediator- and PRDM16 ZF1-dependent manner. Complementary studies show that PRDM16 can enhance *Ucp1* gene expression in a MED1- and TR-dependent manner in cells and also reveal different zinc finger and MED1 domain requirements for PRDM16-dependent activation of *Ucp1* and *Ppargc1a* genes. Overall, our results provide important new insights into PRDM16 function that are of significance with respect to brown and beige fat cell transcription programs.

Results

PRDM16 is recruited to the Ucp1 enhancer via MED1 or PGC-1α in vitro

Previous studies identified a 220-base-pair (bp) enhancer that is responsible for expression of the *Ucp1* gene in brown fat cells and in response to norepinephrine (Kozak et al. 1994). This enhancer is located 2.5 kb upstream of the transcription start site (TSS) and contains binding elements for several factors that include PPARs and TRs (Fig. 1A; Sears et al. 1996; Chen et al. 2009). Since PGC-1α has been shown to interact with TRα/RXRα in a ligand-dependent and LxxLL domain-dependent manner (Chen et al. 2009) and with PRDM16 (Seale et al. 2007), we hypothesized that PRDM16 might be recruited to the enhancer region of the *Ucp1* gene through the interaction with PGC-1α. This possibility was tested in an immobilized template assay with purified proteins and a bead-immobilized DNA fragment spanning the 220-bp *Ucp1* enhancer. As shown in Figure 1B, PRDM16 was recruited to the *Ucp1* enhancer in the presence of TRα/RXRα, TR ligand T3, and PGC-1α (lane 4). Removal of either T3 (Fig. 1B, lane 3), TRα/RXRα (Fig. 1B, lane 6), or PGC-1α (Fig. 1B, lane 2) abolished the recruitment, indicating that PRDM16 is recruited to the enhancer–TRα/RXRα–PGC-1α complex through PGC-1α. Because the Mediator subunit MED1 directly binds to both TRα/RXRα and PGC-1α (Chen et al. 2009), we also investigated whether MED1 might affect PGC-1α-mediated PRDM16 recruitment to the *Ucp1* enhancer. Notably, whereas addition of MED1 with PGC-1α moderately enhanced the recruitment of PRDM16 over the level seen with PGC-1α alone (Fig. 1C, lane 2 vs. lane 4), PRDM16 was efficiently recruited to the *Ucp1* enhancer through MED1 even in the absence of PGC-1α (Fig. 1C, lane 3). A further analysis revealed, as expected, that the MED1-dependent recruitment of PRDM16 is also T3-dependent and TRα/RXRα-dependent (Fig. 1D). Therefore, since MED1 recruitment to the *Ucp1* enhancer is also T3-dependent and TRα/RXRα-dependent (Chen et al. 2009), these results indicate that PRDM16 can be recruited to the enhancer through MED1. Since MED1 is one of the components of the multisubunit Mediator, we next tested whether PRDM16 can be recruited to the enhancer through the complete Mediator complex. As expected, PRDM16 was recruited to the *Ucp1* enhancer in a Mediator- and T3-dependent manner (Supplemental Fig. S1, lanes 1–3). Moreover, similar to what was observed with MED1, the addition of Mediator with

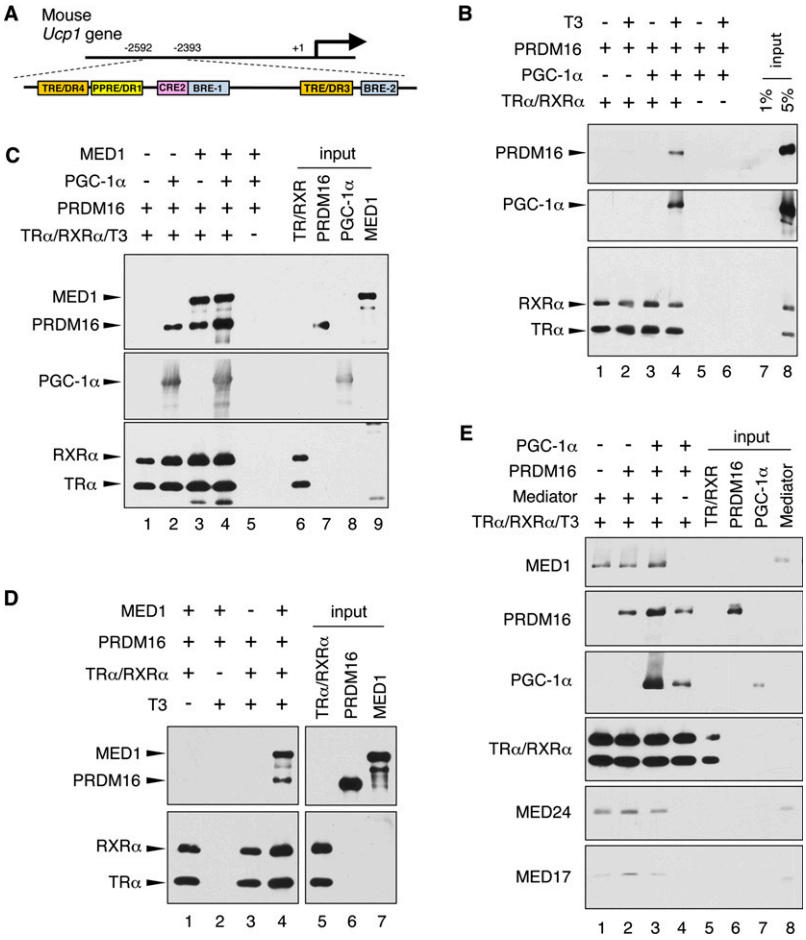

Figure 1. In vitro recruitment of PRDM16 to the *Ucp1* enhancer through PGC-1α or the Mediator subunit MED1. (*A*) Schematic representation of the mouse *Ucp1* gene enhancer. A 200-bp enhancer region extending from −2592 to −2393 relative to the TSS was used in the immobilized template assay. (*B*) Recruitment of PRDM16 to the *Ucp1* enhancer through PGC-1α. Immobilized template assays were carried out as described in the Materials and Methods. Bound proteins in *B–E* were detected by immunoblotting. (*C*) Recruitment of PRDM16 to the *Ucp1* enhancer through MED1 or PGC-1α. (*D*) T3-, TRα/RXRα-, and MED1-dependent recruitment of PRDM16 to the *Ucp1* enhancer. (*E*) Recruitment of PRDM16 through the Mediator complex.

PGC-1α resulted in a significantly higher level of PRDM16 recruitment than observed with either factor alone (Fig. 1E, lane 3 vs. lanes 2 and 4). These results indicate that PRDM16 can be efficiently recruited to the *Ucp1* enhancer by interactions with either TRα/RXRα-bound PGC-1α or the TRα/RXRα-bound MED1/Mediator but also raise the possibility of cooperativity between PGC1α and MED1/Mediator in PRDM16 recruitment.

In an extension of these studies, we observed recruitment of PRDM16 to enhancer-bound PPARγ/RXRα in the presence of MED1 and/or PGC-1α but not when incubated independently with the PPARγ/RXRα–enhancer complex (Supplemental Fig. S2). These results mirror those observed with enhancer-bound TRα/RXRα. In relation to both the PPARγ and TRα studies, which indicate indirect recruitment of PRDM16 to TRα/RXRα–enhancer and PPARγ/RXRα–enhancer complexes, it is noteworthy that direct interactions of PRDM16 with free (unbound) TRα and PPARγ can be demonstrated by GST pull-down assays (Supplemental Fig. S3; Seale et al. 2008). However, while these interactions could be important for the overall stability of PRDM16-containing NR–*Ucp1* enhancer complexes, they do not seem to be sufficient (in the absence of MED1 and/or PGC-1α) for their formation.

In view of the results described above and previous demonstrations of PGC-1α interactions with not only PRDM16 and MED1 (above) but also p300 (Puigserver et al. 1999; Wallberg et al. 2003), we further analyzed the interactions of these components on the *Ucp1* enhancer in the immobilized template assay. As shown in Supplemental Figure S4, p300 was not stably recruited to the TRα–RXRα–enhancer complex either alone (lanes 1–3) or in the presence of MED1. However, as expected, p300 recruitment was effected by PGC-1α (Supplemental Fig. S4, lane 5). p300 was recruited to a similar level along with PRDM16 when PRDM16 was added with PGC-1α (Supplemental Fig. S4, lane 7). Notably, the addition of MED1 with PGC-1α and PRDM16 led to the expected recruitment of MED1 (along with PGC-1α and PRDM16) but, surprisingly, an apparent reduction of p300 (Supplemental Fig. S4, lane 8). These results further suggest a role for PRDM16 in association with MED1/Mediator, which is further analyzed below, as well as the possibility of a PRDM16 function in association with a PGC-1α/p300 enhancer complex or in the transition from this chromatin-modifying complex to the Mediator-containing transcription preinitiation complex.

PRDM16 interacts with the N-terminal region of MED1 through its ZF1 domain

To determine the region of PRDM16 that is responsible for the interaction with MED1, we used in vitro binding

assays with GST-fused PRDM16 fragments (Fig. 2A) and in vitro translated MED1 and PGC-1α. As reported previously (Kajimura et al. 2008), PGC-1α bound to PRDM16 regions containing the N-terminal (ZF1) and C-terminal (ZF2) zinc finger domains (Fig. 2B, middle panel, lanes 2,5). In contrast, MED1 interacted only with the N-terminal zinc finger domain (Fig. 2B, top panel, lane 2). Negative control luciferase proteins did not bind to any fragment of PRDM16 (Fig. 2B, bottom panel). A subsequent in vitro binding assay using purified MED1 and PGC-1α proteins instead of in vitro translated proteins again showed strong interactions of MED1 with the ZF1 domain and of PGC-1α with both the ZF1 and ZF2 domains, firmly establishing that these interactions are direct (Fig. 2C). To further confirm and extend these results, an immobilized template assay with TRα/RXRα, MED1, or PGC-1α and purified PRDM16 mutants that lack ZF1, ZF2, or both (ΔZF1, ΔZF2, and ΔZF1/2, respectively) was used (Fig. 2D). Notably, wild-type PRDM16 (Fig. 2D, lanes 1–3) and ΔZF2 (Fig. 2D, lanes 7–9), but not ΔZF1 (Fig. 2D, lanes 5–7) or ΔZF1/2 (Fig. 2D, lanes 10–12), showed interactions with both MED1 and PGC-1α. These results are fully consistent with the results in Figure 2, B and C, for MED1. However, they are only partially consistent for PGC-1α, since ΔZF2, but not ΔZF1, binds to PGC-1α in the immobilized template assay, which may indicate more stringent binding conditions in the latter assay and stronger binding of PGC-1α to ZF1 than to ZF2. Overall, these results indicate that the ZF1 domain is required for the recruitment of PRDM16 to the *Ucp1* enhancer through MED1 and PGC-1α.

Next, we investigated the PRDM16-interacting region in MED1 using in vitro translated MED1 deletion mutants (Fig. 2E). As shown in Figure 2F, full-length (lane 3),

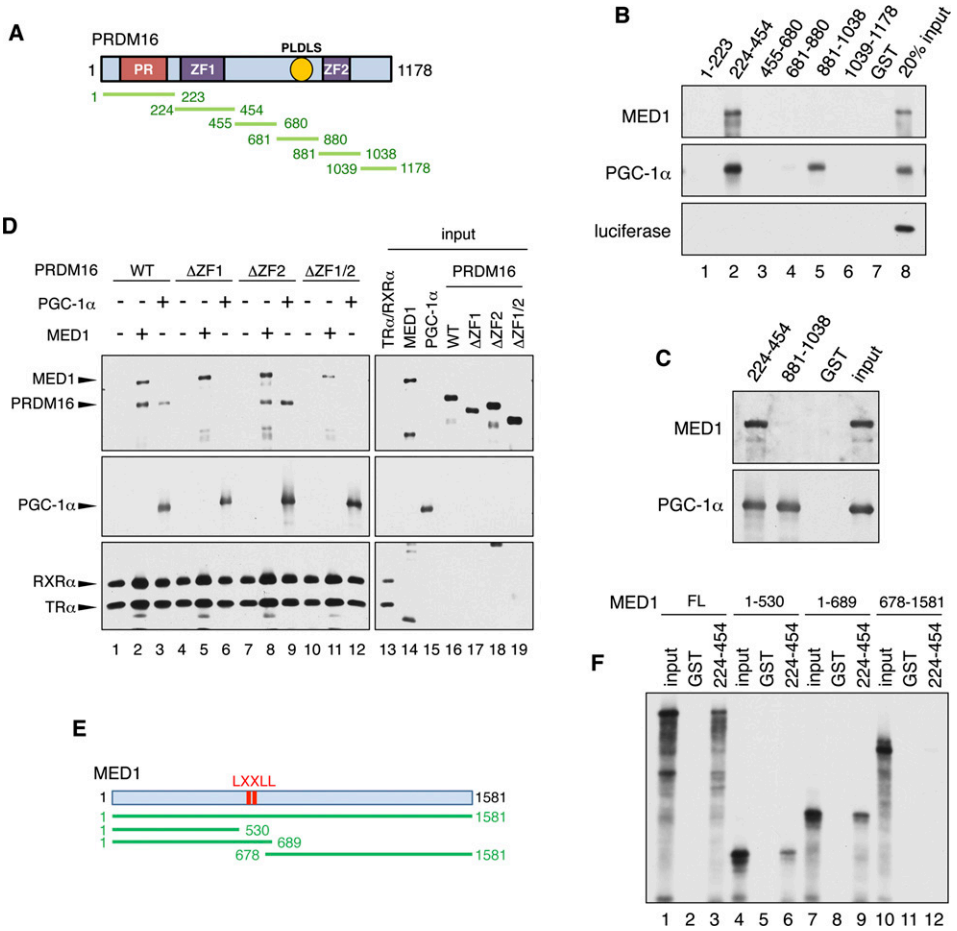

Figure 2. Direct PRDM16–MED1 interaction through the ZF1 domain of PRDM16 and the N-terminal region of MED1. (*A*) Schematic representation of PRDM16 and its truncated mutants. (PR) PR domain; (ZF1) zinc finger domain 1; (ZF2) zinc finger domain 2. (*B*) Interaction of MED1 and PGC-1α with the ZF1 domain of PRDM16. In vitro binding assay was carried out using GST-fused PRDM16 fragments and in vitro translated MED1. (*C*) Direct interaction of MED1 with the ZF1 domain. In vitro binding assay was carried out as in *B* using purified MED1 or PGC-1α instead of in vitro translated proteins. (*D*) Requirement of ZF1 domain for the recruitment of PRDM16 to the *Ucp1* enhancer through MED1 and PGC-1α. Immobilized template assays were performed using the immobilized *Ucp1* enhancer, TRα/RXRα, MED1, PGC-1α, and PRDM16 and its mutants. Bound proteins were detected by immunoblotting. (*E*) Schematic representation of truncated mutants of MED1. (*F*) Interaction of the ZF1 domain with the N-terminal region of MED1. In vitro binding assays were carried out using GST-PRDM16 (224–424) and in vitro translated MED1 mutants.

1–530 (lane 6), and 1–689 (lane 9) MED1 bound to GST-ZF1 (relative to GST), whereas 678–1581 MED1 (lane 12) did not. These results indicate that PRDM16 and MED1 directly interact through the ZF1 domain of PRDM16 and the conserved MED1 N terminus that lacks both of the NR boxes.

PRDM16 enhances TR-driven transcription in vitro

To test whether PRDM16 enhances TR-driven transcription, we used an in vitro transcription assay reconstituted with purified factors (Pol II, GTFs, PC4, and Mediator) (Supplemental Fig. S5) and a naked DNA template that contains five tandem repeats of a TR-binding element (TRE) fused to the adenovirus major late core promoter (AdMLP) (Fig. 3A). As shown in Figure 3B, TRα/RXRα and T3 effected a significant level of transcription (lane 2 vs. lane 1) that was further enhanced by Mediator (lane 6 vs. lane 2). Under these conditions, PRDM16 further enhanced the transcription in a dose-dependent manner (Fig. 3B, lanes 7–11). Notably, transcription activity was significantly decreased in the absence of Mediator (Fig. 3B, lane 11 vs. 12), suggesting that Mediator is critical for the transcriptional enhancement by PRDM16. Consistent with the Mediator requirement, the transcription-enhancing effect of PRDM16 was severely attenuated by deletion of the ZF1 domain that was shown above (Fig. 2C) to interact with MED1 (Fig. 3C, lanes 2,3 vs. lanes 4,5). Surprisingly, since the ΔZF2 mutant was shown above (Fig. 2C) to interact with MED1 and be recruited to the template, deletion of the ZF2 domain also abolished the transcriptional enhancement (Fig. 3C, lanes 6,7). These results indicate that PRDM16 can directly enhance TR-driven transcription in a Mediator-dependent fashion and

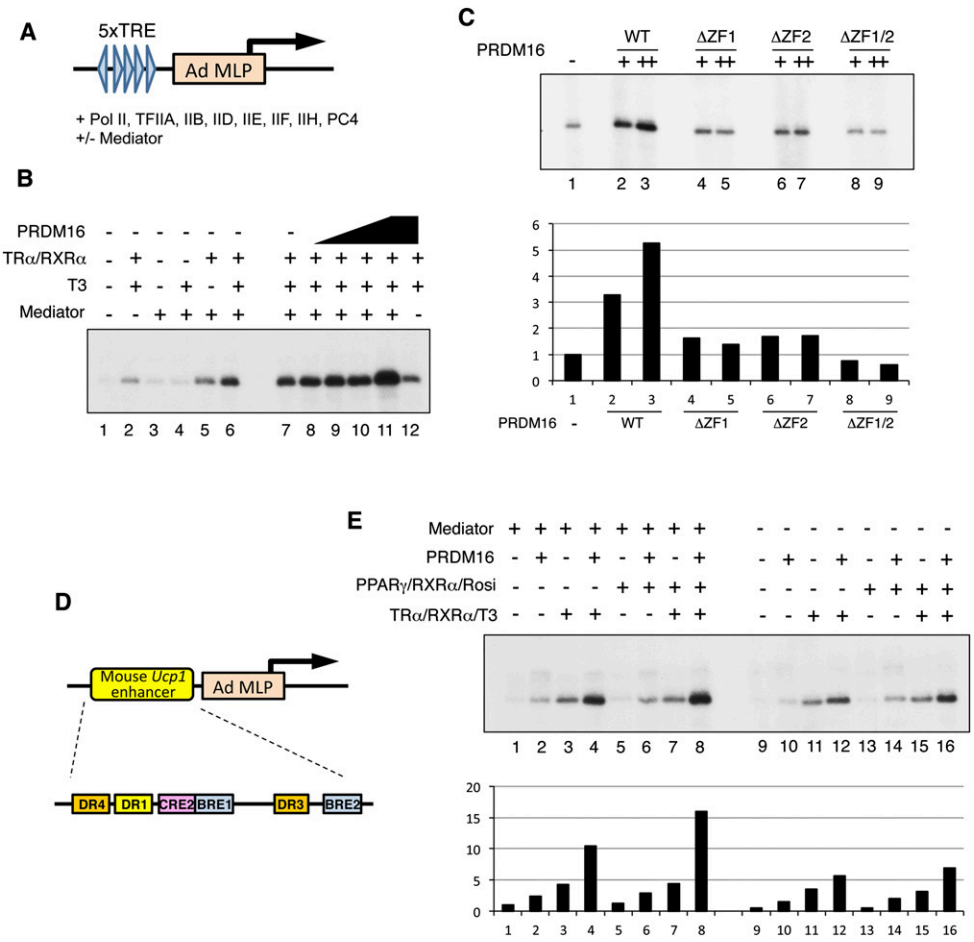

Figure 3. PRDM16 enhancement of TRα/RXRα-dependent transcription in vitro with defined factors. (*A*) Schematic representation of the template used for in vitro transcription assays in *B* and *C*. The template contains five tandem TREs fused to the AdMLP. (*B*) Dose-dependent transcriptional enhancement by PRDM16. Transcription was reconstituted with purified Pol II, GTFs, and PC4 (all reactions) and purified TRα/RXRα, Mediator, and PRDM16 as indicated. (*C*) Requirement of ZF domains for the transcription-enhancing function of PRDM16. In vitro transcription was performed as in *B* with TRα/RXRα/T3 and Mediator and with PRDM16 mutants as indicated. Signal intensities were quantified by phosphorimaging and are represented as bar graphs. (*D*) Schematic representation of the template used for in vitro transcription assays in *E*. The template contains the enhancer region of the *Ucp1* gene fused to the AdMLP. (*E*) In vitro transcription with the *Ucp1* enhancer template and purified factors. Purified TRα/RXRα and PPARγ/RXRα were used as activators. PRDM16 function was tested in the presence (lanes *1–8*) or absence (lanes *9–16*) of Mediator.

that the ZF1 and ZF2 domains are both required for this activity in the defined cell-free system.

To determine whether PRDM16 can enhance transcription through the *Ucp1* enhancer in vitro, we constructed a template with the native *Ucp1* enhancer upstream of the AdMLP (Fig. 3D). As shown in Figure 3E, TRα/RXRα/T3 activated transcription from this template in the presence of Mediator (lane 3 vs. lane 1), and PRDM16 further stimulated this activity (lane 4 vs. lane 3). PPARγ/RXRα/rosiglitazone (PPARγ–ligand) and Mediator showed a lower level of PRDM16-independent transcription than was observed with TRα/RXRα/T3 and Mediator (Fig. 3E, lane 5 vs. lane 3), although this activity was significantly stimulated by PRDM16 (Fig. 3E, lane 6 vs. lane 5). Consistent with these observations and the presence of both TRα and PPARγ-binding sites in the enhancer, the strongest stimulatory effect of PRDM16 on transcription was observed in the presence of PPARγ/RXRα/rosiglitazone and TRα/RXRα/T3 (Fig. 3E, lane 8 vs. lane 7). Importantly, PRDM16-mediated transcription was significantly reduced, albeit not eliminated, in the absence of Mediator (Fig. 3E, lanes 9–16). These results suggest that PRDM16 can enhance transcription directed by the *Ucp1* enhancer and that Mediator-facilitated recruitment of PRDM16 is important for this enhancement. At the same time, the residual Mediator-independent effect of PRDM16 could reflect some function of PRDM16 through NRs and/or the general transcription machinery.

Deletion of zinc finger domains impairs the ability of PRDM16 to induce brown fat-specific genes

Ectopic expression of PPARγ in fibroblasts facilitates their differentiation into adipocytes in conjunction with adipogenic inducers (Rosen et al. 2002). Remarkably, the coexpression of PRDM16 with PPARγ in fibroblasts also activates expression of brown fat-specific genes such as *Ucp1* and *Ppargc1a* upon adipogenic induction (Seale et al. 2007). In order to investigate PRDM16 function in conjunction with Mediator in a cellular context, we first established MEF cells that stably express PRDM16 or its mutants (ΔZF1 and ΔZF2) together with PPARγ and then analyzed gene expression after differentiation into adipocytes. As shown in Figure 4A, expression of PRDM16 or either of the ΔZF mutants did not affect adipogenesis as monitored by Oil Red O staining of triglycerides. Similar expression levels of the common adipose gene *Fabp4* (Fig. 4B) also indicate equivalent differentiation regardless of PRDM16 expression. As reported previously (Seale et al. 2007), PRDM16 induced robust expression of *Ucp1* and *Ppagc1a* in differentiated cells, and expression levels were further enhanced by forskolin, which increases the cellular cAMP concentration (Fig. 4C). Notably, deletion of the ZF1 domain (ΔZF1) completely abolished the induction of *Ucp1* (Fig. 4C, left panel), consistent with the in vitro transcription data in Figure 3C. In contrast, whereas it failed to induce in vitro transcription from the model TRE-containing promoter (Fig. 3C), the ΔZF2 mutant still induced high

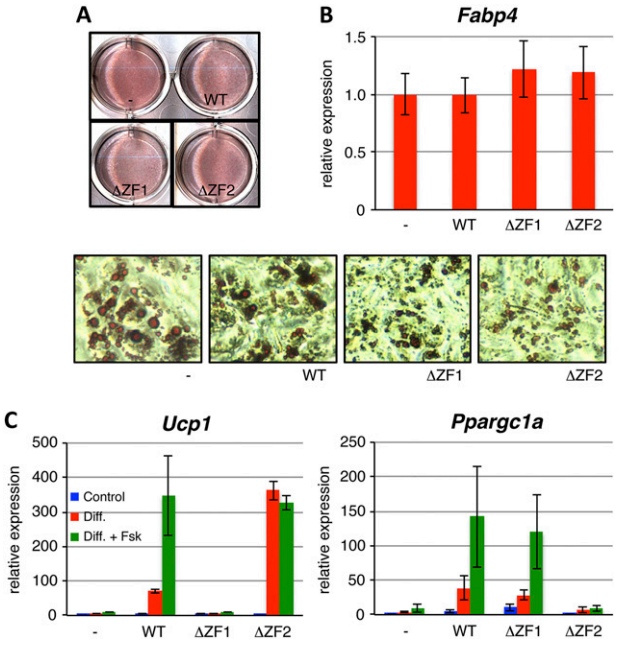

Figure 4. PRDM16 zinc finger domain requirements for PRDM16-dependent expression of brown fat-selective genes in adipocytes. (*A*) Oil Red O staining of MEFs coexpressing PPARγ and PRDM16 or its mutants after adipogenic induction. Differentiation into adipocytes was induced as described in the Materials and Methods. (*B*) Analysis of *Fabp4* gene expression. Total RNA was isolated from differentiated cells, and expression levels were quantified by real-time RT–PCR. (*C*) Analysis of brown fat-specific gene expression, quantified as in *B*. Blue bars show expression in undifferentiated cells, red bars show expression in differentiated cells, and green bars show expression in forskolin (Fsk)-treated cells after differentiation induction. Data are shown as mean ± standard deviation.

levels of *Ucp1* expression in the differentiated cells in both the presence and absence of forskolin (Fig. 4C, left panel). Interestingly, in contrast to the results for *Ucp1*, ΔZF1 induced *Ppagc1a* expression as well as wild-type PRDM16, while ΔZF2 could not do so at all (Fig. 4C, right panel). These results suggest that PRDM16 regulates the expression of *Ucp1* and *Ppagc1a* by at least partially distinct mechanisms related to the different ZF domains in PRDM16 and that the ΔZF1-mediated interaction with MED1 is required for *Ucp1* expression but not for *Ppagc1a* expression. Although we do not yet know the basis for the ΔZF2-induced expression of *Ucp1* in the absence of forskolin, this could reflect an indirect effect of ΔZF2 that would be consistent with our observations (above and below) of differential gene activation specificities for ΔZF1 and ΔZF2.

MED1 is required for optimal PRDM16-induced Ucp1 expression

To further investigate the MED1 requirement for PRDM16-induced *Ucp1* expression, we established *Med1*$^{-/-}$ cells (generated from *Med1*-null mice) (Ge et al. 2002) that stably express PPARγ and PRDM16.

As shown in Figure 5A and consistent with earlier results (Ge et al. 2002), these *Med1*$^{-/-}$ MEFs failed to differentiate into adipocytes regardless of PRDM16 expression. In spite of their inability to differentiate into adipocytes, these PPARγ- and PRDM16-expressing *Med1*$^{-/-}$ MEFs still showed some *Ucp1* expression in response to forskolin treatment (Fig. 5B, left panel). However, the expression level was significantly lower than that in wild-type MEFs treated with forskolin, indicating that MED1 is required for optimum transcriptional activation of the *Ucp1* gene. Like *Ucp1*, *Ppagc1a* was also induced by PRDM16 in these PPARγ- and PRDM16-expressing MEFs following both differentiation and forskolin treatment (Fig. 5B, right panel). Surprisingly, the induction of *Ppagc1a* expression by PRDM16 was not suppressed but instead was somewhat enhanced (especially in the uninduced state) by *Med1* ablation (Fig. 5B). These results indicate that the MED1–PRDM16 interaction is not required for the activation of *Ppargc1a* expression, at least under these conditions, and raise the possibility that MED1 may actually suppress the expression of the *Ppargc1a* gene in normal undifferentiated cells. Overall, our results indicate that optimal PRDM16-mediated induction of *Ucp1*, but not of *Ppargc1a*, requires MED1 and, furthermore, that the PRDM16–MED1 interaction regulates specific gene expression.

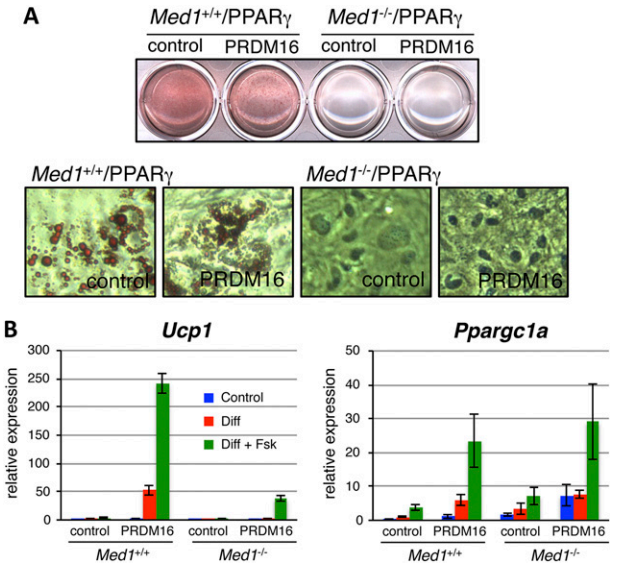

Figure 5. MED1 requirement for normal induction of gene expression by PRDM16 after adipogenic induction. (*A*) Oil Red O staining of wild-type (*Med1*$^{+/+}$) or *Med1*$^{-/-}$ MEFs after induction of adipocyte differentiation. *Med1*$^{+/+}$ or *Med1*$^{-/-}$ cells expressing retroviral PPARγ and either retroviral PRDM16 or vector control were induced for adipocyte differentiation. (*B*) Analysis of *Ucp1* and *Ppargc1a* gene expression. Total RNAs were isolated from cells, and expression levels were quantified by real-time RT–PCR. Blue bars show expression in undifferentiated cells, red bars show expression in differentiated cells, and green bars show expression in forskolin (Fsk)-treated cells after differentiation induction.

PRDM16 in conjunction with forskolin can induce Ucp1 expression in a MED1- and TR-dependent manner in undifferentiated MEFs

Since the cells (MEFs) that are conveniently analyzed for PRDM16 function require treatment with various agents for >1 wk for differentiation induction, many de novo gene expression and chromatin remodeling changes are likely occurring during this period. Furthermore, the failed *Ucp1* induction in *Med1*-null MEFs (Fig. 5B) likely reflects the lack of differentiation and/or factors induced during differentiation. To avoid these complications and establish a more direct involvement of PRDM16 through MED1 in transcriptional activation of *Ucp1*, we used a simplified assay in which the entire differentiation process was omitted. To this end, we established *Med1*$^{+/+}$ and *Med1*$^{-/-}$ MEF cell lines that stably express wild-type or mutant forms of PRDM16. These cells were then treated with forskolin followed by mRNA quantitation by real-time quantitative PCR (qPCR). As shown in Figure 6A, transcription of the *Ucp1* gene was effectively activated in undifferentiated *Med1*$^{+/+}$ MEFs in the presence of PRDM16 and forskolin. Expression of the *Ppargc1a* gene was also induced under these conditions. These results indicate that PRDM16 and forskolin are sufficient to induce the expression of *Ucp1* and *Ppargc1a* in undifferentiated fibroblasts and therefore that this expression is more directly regulated by PRDM16 without an obligatory need for other factors that are induced during differentiation.

Consistent with the results observed in differentiated cells (Fig. 4C), deletion of the ZF1 domain completely abolished the induction of *Ucp1* by PRDM16 in the presence of forskolin while actually enhancing induction of *Ppargc1a* by PRDM16 and forskolin (Fig. 6B). Reciprocally, deletion of the ZF2 domain completely abolished the induction of *Ppargc1a* expression in the presence of forskolin, as observed in differentiated cells (Fig. 4C). However, in contrast to the results in differentiated cells, the induction of *Ucp1* expression in this assay was significantly reduced by deletion of ZF2, suggesting that ZF2 is important for optimal acute expression of the *Ucp1* gene (discussed below) and mimicking the in vitro transcription results (Fig. 3C). These results indicate that, in response to forskolin treatment, the ZF1 and ZF2 domains are both required for optimal *Ucp1* induction in MEFs by PRDM16, while only the ZF2 domain is required for optimal *Ppargc1a* expression.

In order to test the MED1 requirement for PRDM16-induced *Ucp1* and *Ppargc1a* expression, we used the PRDM16-expressing *Med1*$^{-/-}$ MEF cells. As shown in Figure 6C, PRDM16 was much less effective in inducing *Ucp1* expression in *Med1*-null cells, consistent with the immobilized template-binding and in vitro transcription data. Although *Ppargc1a* was already expressed in MED1$^{-/-}$ cells, due to a dramatic (>10-fold) derepression by MED1 ablation, its expression was still markedly (approximately ninefold) increased by PRDM16. To test a TRα dependency on *Ucp1* expression, we used serum that had been T3-depleted (stripped) by charcoal adsorption for

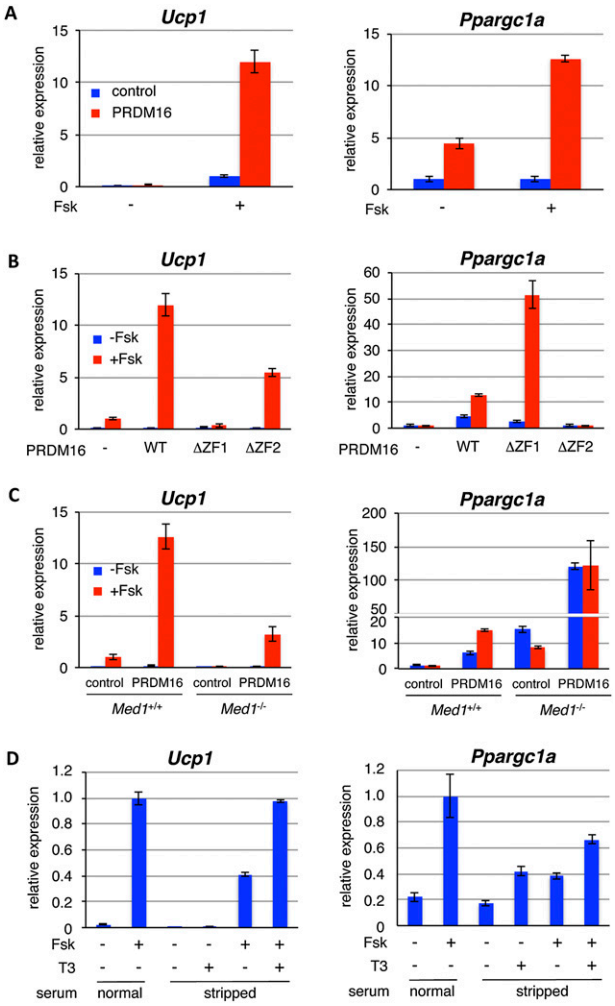

Figure 6. Induction of *Ucp1* expression by forskolin and PRDM16 in fibroblasts dependent on MED1 and TR. (*A*) *Ucp1* and *Ppargc1a* gene expression induced by PRDM16 expression and forskolin treatment in undifferentiated fibroblasts. MEFs were infected by control or PRDM16-expressing retrovirus and then treated with forskolin (Fsk). Gene expression was quantified by real-time RT–PCR. Blue bars show expression in cells infected with control virus, and red bars show expression in cells infected with PRDM16-expressing virus. (*B*) Effect of PRDM16 ZF domain deletions on the induction of *Ucp1* and *Ppargc1a*. MEFs were infected with retroviruses expressing PRDM16 or its mutants and then treated with forskolin for 4 h. Gene expression was analyzed as in *A*. Blue and red bars show expression levels before and after forskolin treatment, respectively. (*C*) MED1 requirement for the induction of *Ucp1* and *Ppargc1a*. *Med1*$^{+/+}$ or *Med1*$^{-/-}$ MEFs were infected with control or PRDM16-expressing retroviruses. (*D*) Contribution of TR to the induction of *Ucp1* and *Ppargc1a*. PRDM16-expresing virus-infected MEFs were cultured in medium containing normal or charcoal-treated (stripped) serum. mRNA expression levels were quantified following treatment with T3, forskolin, or both.

cell culture. Under these conditions with PRDM16-expressing cells, forskolin induced *Ucp1* expression about threefold less effectively than when cells were grown in medium containing normal serum, and the induction was fully restored by readdition of T3 to the serum (Fig. 6D). Expression of the *Ppargc1a* gene was also reduced by T3 depletion, although it was not fully restored by addition of T3. Because activated charcoal adsorbs other hormones as well as T3, this partial recovery of *Ppargc1a* expression suggests that other hormones are involved in the regulation of *Ppargc1a* expression. These results indicate that the robust PRDM16- and forskolin-induced expression of the *Ucp1* gene in undifferentiated cells is mediated by TR and MED1, whereas expression of *Ppargc1a* in these cells does not require MED1.

Although our results have clearly shown roles for TRα and MED1 in PRDM16-dependent transcription of *Ucp1* in undifferentiated fibroblasts, our biochemical studies (above) and previous cell-based studies (above) raised the question of whether PPARγ and PGC-1α may also play significant roles in PRDM16- and forskolin-dependent activation of *Ucp1* in these cells. Notably, however, PRDM16- and forskolin-dependent activation of *Ucp1* was not markedly reduced by either concentrations of the PPARγ antagonist GW9662 that effectively inhibited activation of PPARγ target genes or the knockdown of PGC-1α (data not shown). These results suggest that (1) in agreement with the in vitro transcription data, TRα has an intrinsic ability to facilitate PRDM16-dependent transcription without PPARγ, and (2) along with the *Med1*$^{-/-}$ cell results, PRDM16 may act mainly in conjunction with MED1 rather than PGC-1α to facilitate *Ucp1* expression in undifferentiated MEFs. However, these results do not rule out roles for PPARγ and PGC-1α, potentially cooperative with TRα and MED1, respectively, in PRDM16-dependent transcription in other scenarios and cell types. They also do not exclude a potential role for PGC-1β in conjunction with MED1 in the absence of PGC-1α.

PRDM16 is recruited to the enhancer region of the Ucp1 gene in cells

To determine whether PRDM16 is recruited to the enhancer following *Ucp1* induction, we treated *Med1*$^{+/+}$ MEFs that stably express PPARγ and PRDM16 with forskolin and performed a chromatin immunoprecipitation (ChIP) assay with an antibody specific for PRDM16. As reported previously (Kajimura et al. 2009), PRDM16 bound to the TSS of *Ppargc1a* but not to a region 7 kb upstream of the TSS (Fig. 7A). Under these conditions, PRDM16 also bound to both the enhancer and the TSS of the *Ucp1* gene but not to a region 5 kb downstream from the TSS (Fig. 7B). In order to assess a role for MED1 in the recruitment of PRDM16, we similarly analyzed *Med1*$^{-/-}$ MEF cells that stably express both PPARγ and PRDM16. Binding of PRDM16 to the *Ppargc1a* TSS in *Med1*$^{-/-}$ cells was very similar to that in wild-type cells (Fig. 7A), indicating MED1-independent recruitment of PRDM16 to *Ppargc1a* and consistent with the functional studies indicating MED1-independent *Ppargc1a* expression. In contrast, PRDM16 occupancy at the *Ucp1* enhancer and TSS was significantly decreased in the absence of MED1 (Fig. 7B). However, the residual binding of PRDM16 in

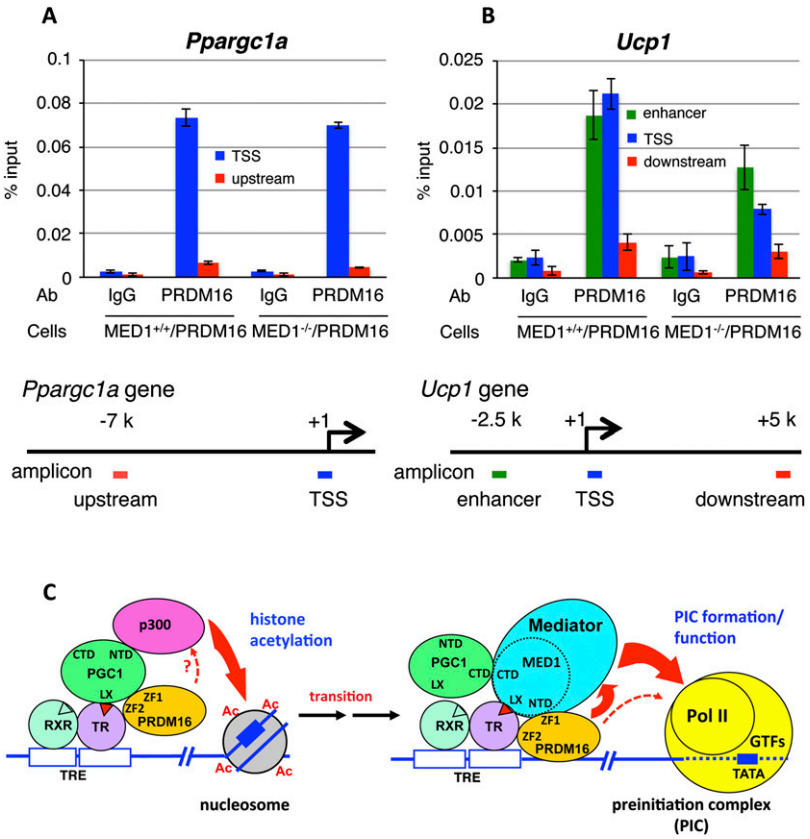

Figure 7. Recruitment of PRDM16 to *Ucp1* and *Ppargc1a* genes. (*A*,*B*) ChIP assays for PRDM16 binding to *Ppargc1a* (*A*) and *Ucp1* (*B*). *Med1*$^{+/+}$ or *Med1*$^{-/-}$ MEFs were treated with forskolin, and ChIP assays were performed with antibodies to PRDM16 or control IgG as indicated. Precipitated DNA was quantified by real-time qPCR using primers targeting the TSS (blue) and upstream (red) regions of *Ppargc1a* (*A*) and the enhancer (green), TSS (blue), and downstream (red) regions of *Ucp1* (*B*). (*C*) Multistep model for activation of target gene *Ucp1* transcription by PRDM16. In an initial series of reactions, liganded enhancer-bound NRs in chromatin templates are recognized by PGC-1α. Bound PGC-1α then recruits both p300, leading to histone acetylation, and PRDM16, which may facilitate p300 function. In a second series of reactions after chromatin remodeling, PGC-1α is displaced from the NR by MED1/Mediator. Through new interactions with MED1, PRDM16 (and possibly PGC-1α) remains associated with the enhancer–NR–Mediator complex and facilitates Mediator functions in the formation and/or function of the preinitiation complex. For additional details, see the text.

Med1$^{-/-}$ cells was greater at the enhancer than at the TSS. Because *Ppargc1a* expression is markedly enhanced in the *Med1*$^{-/-}$ cells (Fig. 6C) and in view of our demonstration of PRDM16 binding to enhancer-bound PGC-1α in the absence of MED1 in vitro (Fig. 1), this residual recruitment of PRDM16 might possibly be mediated by the elevated PGC-1α. Overall, these results suggest that recruitment of PRDM16 to the *Ucp1* TSS is more dependent on MED1, while recruitment to the enhancer may be facilitated by both MED1 and PGC-1α. The MED1-enhanced recruitment of PRDM16 to the *Ucp1* gene is consistent with the demonstrated MED1 requirement for *Ucp1* expression, although MED1–PRDM16 interactions could affect steps in transcription other than PRDM16 recruitment per se.

Discussion

The central role of PRDM16 as a determinant of brown and beige fat phenotypes underscores the importance of an understanding of its molecular mechanisms of action in the activation and repression of specific genes. In this study, we confirm that the brown fat-specific *Ucp1* gene is directly regulated by PRDM16 and, most importantly, provide new mechanistic insights into PRDM16 function. Our biochemical studies show unequivocally that (1) PRDM16, through its ZF1 domain, directly interacts with the Mediator coactivator complex through the N-terminal region of the MED1 subunit; (2) PRDM16 can be recruited to the *Ucp1* enhancer through interactions with either TRα/RXRα-bound MED1 or TRα/RXRα-bound PGC-1α; and (3) PRDM16 can enhance TR-mediated transcription in a biochemically defined system in a Mediator-dependent manner. These studies provide the first link of PRDM16 through the Mediator to the general transcriptional machinery. Complementary cell-based assays establish that (1) PRDM16 enhances *Ucp1* transcription dependent on MED1 and TR in undifferentiated fibroblasts in response to forskolin treatment, and (2) PRDM16 is recruited in a MED1-enhanced manner to the *Ucp1* enhancer and TSS. In conjunction with data from other studies of MED1, PGC-1α, and p300 (Chen et al. 2009), our in vitro results lead to a multistep model for PRDM16 function on the *Ucp1* gene that is shown in Figure 7C and detailed below. Our results also indicate gene-selective functions of MED1 as well as individual PRDM16 zinc finger domains in gene activation by PRDM16.

Transcriptional enhancement by PRDM16 mediated by direct interactions with MED1/Mediator

Our analyses with purified wild-type and mutant proteins have unequivocally established direct PRDM16–MED1 interactions that minimally involve the ZF1 domain of PRDM16 and the N-terminal domain of MED1 and also confirmed direct PRDM16–PGC-1α interactions through the ZF1 and ZF2 domains. Analyses in the more physi-

ological context of TRα/RXRα–*Ucp1* enhancer complexes established comparable levels of PRDM16 recruitment through these interactions by either enhancer-bound MED1/Mediator or enhancer-bound PGC-1α as well as potential cooperativity between MED1/Mediator and PGC-1α in PRDM16 recruitment. PRDM16 was also shown to enhance TR-driven transcription in an in vitro system reconstituted with purified factors and a naked DNA template, thus indicating direct functions on transcription independent of potential PRDM16 functions (below) through histone-modifying factors. Importantly, the PRDM16-enhanced transcription was heavily dependent on both Mediator and the MED1-interacting ZF1 domain in PRDM16. These results indicate that recruitment of PRDM16 to the enhancer–TRα/RXRα–Mediator complex through the MED1 interaction is required for the transcription-enhancing activity of PRDM16. Given the well-established role of the Mediator through interactions with Pol II and TFIID in preinitiation complex assembly and function (Malik and Roeder 2010), these results indicate an ultimate effect of PRDM16 at the level of the preinitiation complex.

Consistent with the in vitro results, either *Med1* ablation or a ZF1 deletion in PRDM16 strongly suppresses the robust induction of *Ucp1* by PRDM16 in undifferentiated MEFs in response to forskolin. Furthermore, PRDM16 recruitment to the *Ucp1* gene is decreased in *Med1*-null MEFs. These results suggest that the PRDM16–MED1 interaction is required for optimal *Ucp1* gene expression in MEFs. Interestingly, PRDM16 recruitment to the *Ucp1* enhancer is reduced less severely than recruitment to the *Ucp1* promoter in *Med1*-null cells. This residual PRDM16 recruitment to the enhancer in *Med1*-null cells is likely mediated by PGC-1α in view of our demonstration of an elevated level of PGC-1α in *Med1*-null cells and the ability of enhancer–TRα/RXRα-bound PGC-1α to efficiently recruit PRDM16 in vitro. These results suggest that substantial PRDM16 recruitment to the enhancer through PGC-1α or possibly other factors, including NRs themselves (Seale et al. 2008), is not sufficient and that the PRDM16 interaction with MED1/Mediator is necessary for normal expression of *Ucp1*. Thus, at least part of the effect of PRDM16 must involve its effect through Mediator on the preinitiation complex.

Possible PRDM16 coactivator function through PGC-1α

NR-bound PGC-1α has been reported to enhance transcription by recruiting p300 to target genes and/or facilitating preinitiation complex formation through interaction with MED1 (Puigserver et al. 1999; Wallberg et al. 2003; Chen et al. 2009). Our demonstration that PRDM16 can be recruited through interaction of its ZF1 domain with PGC-1α to the *Ucp1* enhancer–TRα/RXRα–PGC-1α complex in vitro is consistent with previous studies (Seale et al. 2007) indicating that PRDM16 function is mediated at least in part through a PGC-1α interaction (albeit by a somewhat different mechanism). Consistent with our in vitro results and despite the expression of *Ppargc1a*, *Ucp1* expression is not induced by forskolin in MEFs (differentiated or undifferentiated) that express the PRDM16 ΔZF1 mutant that cannot bind enhancer-bound PGC-1α. Although this could also reflect the lack of binding to enhancer-bound MED1/Mediator, evidence for this second proposed function of PRDM16 through PGC-1α is provided by the observation that PRDM16-expressing *Med1*-null MEFs, which show markedly elevated *Ppargc1a* expression, still show both a weak (but significant) induction of *Ucp1* transcription (Fig. 6C) and residual PRDM16 recruitment to the enhancer in response to forskolin (Fig. 7B). Overall, the results suggest that, under some conditions, PRDM16 and PGC-1α can act together, possibly with the PGC-1α-interacting p300, to partially activate *Ucp1* transcription, while the PRDM16-MED1/Mediator interaction is required for full transcriptional activation. The minimal effect of reduced *Ppargc1a* expression relative to the major effect of *Med1* ablation also reveals a dominant role for MED1 in PRDM16-dependent *Ucp1* activation in MEFs.

It deserves mention that while PRDM16 and/or the derived ZF1 domain have been reported to interact directly with unbound PPARγ (Seale et al. 2008), as we confirmed here for TRα and PPARγ, we failed to observe PRDM16 recruitment to the *Ucp1* enhancer through a direct interaction with PPARγ or TRα in our immobilized template assay. These observations, along with the PGC-1α-dependent recruitment of PRDM16 in this assay, suggest that PRDM16 may be recruited to the *Ucp1* gene through PGC-1α in the *Med1*-null MEFs but do not exclude alternative recruitment mechanisms (e.g., through PPARγ and other associated factors). In adipocytes, *Ucp1* is activated by not only PPARγ and TRα in conjunction with PGC-1α (Puigserver et al. 1998) but also other DNA-binding activators that include ATF-2 (Cao et al. 2004; Collins et al. 2010). These observations and our current results lead us to suggest that PRDM16 may facilitate PGC-1α- and p300-dependent chromatin remodeling even in the absence of MED1, especially at the elevated PGC-1α levels resulting from MED1 loss, and that factors such as ATF-2 may activate transcription of *Ucp1* in this situation. However, as emphasized above, our study strongly suggests that TR and MED1 are also required for optimum PRDM16-dependent expression of the *Ucp1* gene.

PRDM16-induced Ucp1 expression requires PKA activation

PRDM16 has been shown to strongly enhance the cAMP-induced expression of *Ucp1* (and other genes) in adipocytes (Seale et al. 2007). In this study, we found that ectopic PRDM16 expression and forskolin treatment are sufficient for robust *Ucp1* expression in fibroblasts even without differentiation into adipocytes. This finding allowed us to more directly analyze the MED1 and PRDM16 domain requirements for PRDM16 function. In this assay, PRDM16 expression in the absence of forskolin induces only weak expression of *Ucp1*, in agreement with a previous report (Seale et al. 2007) that forskolin-induced cAMP-dependent protein kinase (PKA) activation is

required for PRDM16-dependent enhancement of *Ucp1* expression. Although ATF-2 may also contribute to *Ucp1* expression, our demonstration that *Med1* ablation and T3 depletion severely attenuate forskolin-dependent *Ucp1* induction indicates that MED1/Mediator and TR play central roles, along with PRDM16, in regulating transcription of *Ucp1* under β-adrenergic signaling. Although the mechanisms by which PRDM16 is activated under β-adrenergic signaling are not yet known, possibilities include covalent modification of PRDM16 (e.g., by phosphorylation) and synergy between PRDM16 and β-adrenergic signaling to remove factors such as LXR and RIP140 that repress the steady-state expression of *Ucp1* (Leonardsson et al. 2004; Kalaany et al. 2005).

Interestingly, several other brown adipocyte-selective genes, such as *Cidea* and *Dio2*, were not induced by PRDM16 and forskolin treatment in fibroblasts (data not shown), possibly because differentiation to adipocytes is required for their expression. In beige fat cells, *Ucp1* expression is low in steady state but acutely induced in response to cAMP stimulation (Wu et al. 2012, 2013). We suggest that our forskolin- and PRDM16-dependent induction of *Ucp1* in fibroblasts may mimic, at least in part, this beige fat cell state. Supporting this speculation, it was shown recently that PRDM16 ablation markedly inhibits *Ucp1* expression in beige adipocytes but has minimal effects on *Ucp1* expression in brown adipocytes (Cohen et al. 2014). Since UCP1 plays a central role in the thermogenic functions of brown and beige fat cells, rapid induction of *Ucp1* may be necessary for an effective response to cold exposure, and PRDM16 may contribute to this acute expression of *Ucp1*.

Conditional requirement for the ZF2 domain in PRDM16-dependent transcription

Although PRDM16 lacking the ZF2 domain (ΔZF2) can be recruited to the template through the MED1–ZF1 domain interaction (Fig. 2D), the ZF2 domain is required for the transcriptional stimulatory activity of PRDM16 in the in vitro transcription assay (Fig. 3C). The fact that this assay contained only a limited set of well-defined general transcription factors raises the possibility of a secondary PRDM16–ZF2 interaction with one of these factors (e.g., Pol II or a GTF) that complements the ZF1–MED1/Mediator interaction to facilitate preinitiation complex formation or function. Alternatively, there may be a ZF2–MED1/Mediator interaction that was not detected in the stringent binding assays with purified proteins or a secondary stabilizing interaction of ZF2 with NRs (Seale et al. 2008). Consistent with the in vitro transcription results, the ZF2 domain contributes significantly to *Ucp1* induction by PRDM16 in response to forskolin treatment in fibroblasts (Fig. 6B). However, ZF2-deficient PRDM16 is as effective as wild-type PRDM16 in the induction of *Ucp1* expression in differentiated adipocytes (Fig. 4C). In this latter case, the ZF2 domain requirement might be circumvented by other compensatory factors induced during the differentiation process. From the above results, the ZF2 domain seems to be selectively required for acute expression of the *Ucp1* gene, as, for example, in *Ucp1* induction in response to β-adrenergic stimulation of beige fat cells (Wu et al. 2012).

Multistep model for induction of Ucp1 transcription by PRDM16

From this study, we propose a multistep model (Fig. 7C) for *Ucp1* activation by PRDM16 as follows. Through a direct interaction with NR-bound PGC-1α, PRDM16 is recruited to an NR–PGC-1α–enhancer complex (Fig. 1) or, more likely, an NR–PGC-1α–p300–enhancer complex (Supplemental Fig. S4) within chromatin, where it may potentially stabilize the PGC-1α–p300 interaction and enhance chromatin remodeling (histone acetylation) by p300. After p300-mediated chromatin remodeling, PGC-1α is displaced from the NR interaction site by the stronger MED1–NR interaction (Chen et al. 2009). Formation of a new NR–Mediator–enhancer complex may be accompanied by loss of p300 but retention of PRDM16 and (potentially) PGC-1α (Supplemental Fig. S4) through interactions with the MED1 N-terminal domain (Fig. 2) and the MED1 C-terminal domain (Chen et al. 2009), respectively. As shown in the present study (Fig. 3), PRDM16 acts cooperatively with Mediator to enhance transcription by the factors that form the preinitiation complex. As depicted in Figure 7C (solid red arrows), PRDM16 may directly enhance the function of the Mediator (which interacts with Pol II and TFIID) (Malik and Roeder 2010) in preinitiation complex formation/function. As discussed above, PRDM16 might also act directly (through ZF2) on the preinitiation complex (Fig, 7C, dashed red arrow). In presenting this model, we note that it is based primarily on biochemical assays with purified factors and is supported by functional assays in MEFs involving acute induction of *Ucp1* by forskolin and thus does not exclude other complementary mechanisms—such as the recruitment or stabilization of MED1/Mediator by transcription factor-bound PRDM16—that may be used in other cell types and signaling pathways. In this regard, we note that whereas we could not detect direct PRDM16 binding to *Ucp1* enhancer-bound NRs (Fig. 1; Supplemental Fig. S1, S2), our biochemical demonstration of direct PRDM16–TRα and PRDM16–PPARγ interactions in the absence of DNA (Supplemental Fig. S3) leaves open the possibility that such interactions may in some situations contribute to either the primary recruitment or the stabilization (Fig. 7C) of cofactors such as MED1/Mediator or PGC-1α.

Interestingly, the PRDM16- and forskolin-induced expression of *Ppargc1a* in undifferentiated fibroblasts was found to be independent of MED1 and ZF1 but dependent on ZF2, indicating an activation mechanism distinct from that used for *Ucp1*. In this regard, it has been reported that PRDM16 can interact directly with several transcription (co)factors other than PGC-1α and MED1 (Kajimura et al. 2008, 2009; Seale et al. 2008; Ohno et al. 2013) and that it has both intrinsic DNA-binding (Nishikata et al. 2003) and histone methyltransferase (Pinheiro et al. 2012) activities. These observations suggest that, in addition to

the MED1-mediated function reported here, still other PRDM16 functions and mechanisms remain to be uncovered. The further identification of direct PRDM16 target genes, beyond the very few established thus far, will also help in understanding additional PRDM16 functions and mechanisms.

Materials and methods

Protein purification

Pol II, GTFs, PC4, and Mediator were purified as described previously (Malik and Roeder 2003). Recombinant PRDM16, MED1, TRα, RXRα, PPARγ, and p300 proteins were expressed in Sf9 cells using the Bac-to-Bac baculovirus expression system (Invitrogen) and affinity-purified through Flag tags attached at N termini using M2 agarose. His-tagged PGC-1α was expressed in bacteria and purified as described (Chen et al. 2009).

Immobilized template assay

Immobilized template assays were performed as described (Chen et al. 2009). A mouse *Ucp1* enhancer fragment was prepared by PCR using biotinylated oligonucleotides and immobilized on streptavidin-conjugated magnetic beads (Dynabeads M280 streptavidin, Invitrogen). After incubating the beads in blocking buffer (50 mM Tris-HCl at pH 7.5, 100 mM KCl, 0.01% NP-40, 1 mg/mL BSA, 0.5 mM PMSF, 10 mM DDT, 10 μg/mL salmon sperm DNA [GE Healthcare], 10 μg/mL poly dI–dC [Roche]), purified proteins were added to the reaction and incubated for 30 min at room temperature. The beads were then washed with wash buffer (50 mM Tris-HCl at pH 7.5, 100 mM KCl, 0.01% NP-40, 0.5 mM PMSF, 0.5 mM DTT) three times, and the bound proteins were eluted by boiling in 1× Laemmli sample buffer and analyzed by immunoblot. The standard 100-μL reaction contained 5 μL of beads, 400 ng of DNA fragment, 40 ng of TRα, 40 ng of RXRα, 40 ng of PPARγ, 400 ng of MED1, 400 ng of PGC-1α, and 400 ng of PRDM16.

In vitro binding assays

In vitro protein binding assays were performed as described (Malik et al. 2004). GST-fused PRDM16 fragments were immoblilized on Glutathione Sepharose beads (GE Healthcare) and incubated with in vitro translated ^{35}S-labeled MED1 proteins prepared using the TNT Quick-Coupled transcription/translation system (Promega) in binding buffer (20 mM Tris-HCl at pH 7.5, 10% glycerol, 0.2 mM EDTA, 100 mM KCl, 3 mg/mL BSA, 0.5 mM DTT, 0.5 mM PMSF, 0.1% NP-40) for 4 h at 4°C. The beads were washed with wash buffer (20 mM Tris-HCl at pH 7.5, 0.1 mM EDTA, 20% glycerol, 300 mM KCl, 0.5 mM DTT, 0.5 mM PMSF, 0.1% NP-40). Bound proteins were eluted by boiling in 1× Laemmli sample buffer, separated by SDS-PAGE, and analyzed by autoradiography.

In vitro transcription

In vitro transcription was performed with purified factors as described previously (Malik and Roeder, 2003).

Cell culture

Wild-type and *Med1*$^{-/-}$ MEF cells were established previously (Ge et al. 2002). MEF and HEK293T cells were cultured in DMEM containing 10% fetal bovine serum.

For retrovirus production, HEK293T cells were transfected with pEcotropic plasmid and retrovirus vectors by TransIT (Mirus) and then cultured for an additional 24 h at 32°C. For retrovirus infection, cells were incubated with virus-containing supernatant with 10 μg/mL polybrene for 30 min at 32°C and then centrifuged at 1000*g* for 30 min at room temperature. Medium was changed after the centrifugation, and the cells were cultured for 2 d at 37°C.

For adipocyte differentiation, confluent cells were cultured in medium containing 0.5 mM isobutylmethylxanthine (Sigma), 125 nM indomethacin (Sigma), 1 μM dexamethasone (Sigma), 850 nM insulin (Sigma), 1 nM T3 (Sigma), and 1 μM rosiglitazone (Cyman Chemicals) for 2 d. Next, cells were switched to medium containing 850 nM insulin, 1 nM T3, and 1 μM rosiglitazone. At 6 d after induction, cells were stained with Oil Red O (Sigma) or subjected to RNA extraction for mRNA analysis. For induction of *Ucp1* gene expression, differentiated cells were treated with 10 μM forskolin (Sigma) for 4 h.

Gene expression analysis

Total RNA was prepared using the RNeasy minikit and RNase-free DNase set (Qiagen). RNA was reverse-transcribed using SuperScript III first strand synthesis system for RT–PCR (Invitrogen) following the manufacturer's instructions. Quantitative real-time PCR was performed using SYBR Green master mix (Applied Biosystems). mRNA expression levels were quantified by comparisons with standard curves generated with the plasmids containing PCR target sequences. TATA-binding protein (*Tbp*) was used as an internal control for normalization. PCR reactions were done in triplicate, and data are shown as relative expression. Primer sequences used for real-time PCR are described in Supplemental Table 1.

ChIP assay

Cells were double-cross-linked with 2 mM EGS for 30 min and then 1% formaldehyde for 5 min. Cells were lysed in RIPA0 (10 mM Tris-HCl at pH 7.5, 1 mM EDTA, 0.1% SDS, 1% Triton X-100, 0.1% deoxycholate) containing, in addition, 0.25% Sarkosyl, 1 mM DTT, and 1× protease inhibitor (Calbiochem), and chromatin was solubilized and sheared by sonication. NaCl (5 M) was added to solubilized chromatin recovered after centrifugation to a final concentration of 0.3 M. The solubilized chromatin was incubated with anti-PRDM16 antibody (SDIX) immobilized on protein G-conjugated magnetic beads (Dynabeads Protein G, Invitrogen) for 6 h at 4°C. The beads were washed sequentially (twice each) with RIPA0.3 (RIPA0 containing 0.3 M NaCl), RIPA0, LiCl wash buffer (10 mM Tris-HCl at pH 7.5, 1 mM EDTA, 250 mM LiCl, 0.5% NP-40, 0.5% deoxycholate), and TE buffer (pH 8.0). Next, beads were incubated with elution buffer (50 mM Tris-HCl at pH 7.5, 10 mM EDTA, 1% SDS) for 6 h at 65°C. After treatment with RNase A and Proteinase K, the eluates were purified using ChIP DNA Clean and Concentrator (Zymo Research). Precipitated DNA was quantified by real-time PCR as described above. PCR was done in triplicate, and data are shown as percentage of input. Primers used for real-time PCR are described in Supplemental Table 2.

Acknowledgments

We are grateful to Bruce Spiegelman, Patrick Seale, and Paul Cohen for PRDM16 expression and adenoviral PGC-1α shRNA vectors; Sohail Malik, Miki Jishage, and Neri Minsky for critical reading of the manuscript; and Miho Shimada for technical

advice. This work was supported by National Institutes of Health grant DK071900 to R.G.R.

References

Cannon B, Nedergaard J. 2004. Brown adipose tissue: function and physiological significance. *Physiol Rev* **84:** 277–359.

Cao W, Daniel KW, Robidoux J, Puigserver P, Medvedev AV, Bai X, Floering LM, Spiegelman BM, Collins S. 2004. p38 mitogen-activated protein kinase is the central regulator of cyclic AMP-dependent transcription of the brown fat uncoupling protein 1 gene. *Mol Cell Biol* **24:** 3057–3067.

Chen W, Roeder RG. 2011. Mediator-dependent nuclear receptor function. *Semin Cell Dev Biol* **22:** 749–758.

Chen W, Yang Q, Roeder RG. 2009. Dynamic interactions and cooperative functions of PGC-1α and MED1 in TRα-mediated activation of the brown-fat-specific UCP-1 gene. *Mol Cell* **35:** 755–768.

Cohen P, Levy JD, Zhang Y, Frontini A, Kolodin DP, Svensson KJ, Lo JC, Zeng X, Ye L, Khandekar MJ, et al. 2014. Ablation of PRDM16 and beige adipose causes metabolic dysfunction and a subcutaneous to visceral fat switch. *Cell* **156:** 304–316.

Collins S, Yehuda-Shnaidman E, Wang H. 2010. Positive and negative control of Ucp1 gene transcription and the role of β-adrenergic signaling networks. *Int J Obes (Lond)* **34:** S28–S33.

Fondell JD. 2013. The Mediator complex in thyroid hormone receptor action. *Biochim Biophys Acta* **1830:** 3867–3875.

Fondell JD, Ge H, Roeder RG. 1996. Ligand induction of a transcriptionally active thyroid hormone receptor coactivator complex. *Proc Natl Acad Sci* **93:** 8329–8333.

Ge K, Guermah M, Yuan CX, Ito M, Wallberg AE, Spiegelman BM, Roeder RG. 2002. Transcription coactivator TRAP220 is required for PPARγ 2-stimulated adipogenesis. *Nature* **417:** 563–567.

Glass CK, Rosenfeld MG. 2000. The coregulator exchange in transcriptional functions of nuclear receptors. *Genes Dev* **14:** 121–141.

Harms M, Seale P. 2013. Brown and beige fat: development, function and therapeutic potential. *Nat Med* **19:** 1252–1263.

Kajimura S, Seale P, Tomaru T, Erdjument-Bromage H, Cooper MP, Ruas JL, Chin S, Tempst P, Lazar MA, Spiegelman BM. 2008. Regulation of the brown and white fat gene programs through a PRDM16/CtBP transcriptional complex. *Genes Dev* **22:** 1397–1409.

Kajimura S, Seale P, Kubota K, Lunsford E, Frangioni JV, Gygi SP, Spiegelman BM. 2009. Initiation of myoblast to brown fat switch by a PRDM16-C/EBP-β transcriptional complex. *Nature* **460:** 1154–1158.

Kajimura S, Seale P, Spiegelman BM. 2010. Transcriptional control of brown fat development. *Cell Metab* **11:** 257–262.

Kalaany NY, Gauthier KC, Zavacki AM, Mammen PP, Kitazume T, Peterson JA, Horton JD, Garry DJ, Bianco AC, Mangelsdorf DJ. 2005. LXRs regulate the balance between fat storage and oxidation. *Cell Metab* **1:** 231–244.

Kozak UC, Kopecky J, Teisinger J, Enerback S, Boyer B, Kozak LP. 1994. An upstream enhancer regulating brown-fat-specific expression of the mitochondrial uncoupling protein gene. *Mol Cell Biol* **14:** 59–67.

Leonardsson G, Steel JH, Christian M, Pocock V, Milligan S, Bell J, So PW, Medina-Gomez G, Vidal-Puig A, White R, et al. 2004. Nuclear receptor corepressor RIP140 regulates fat accumulation. *Proc Natl Acad Sci* **101:** 8437–8442.

Lin J, Wu PH, Tarr PT, Lindenberg KS, St-Pierre J, Zhang CY, Mootha VK, Jager S, Vianna CR, Reznick RM, et al. 2004. Defects in adaptive energy metabolism with CNS-linked hyperactivity in PGC-1α null mice. *Cell* **119:** 121–135.

Lonard DM, O'Malley BW. 2006. The expanding cosmos of nuclear receptor coactivators. *Cell* **125:** 411–414.

Malik S, Roeder RG. 2003. Isolation and functional characterization of the TRAP/mediator complex. *Methods Enzymol* **364:** 257–284.

Malik S, Roeder RG. 2010. The metazoan Mediator co-activator complex as an integrative hub for transcriptional regulation. *Nat Rev Genet* **11:** 761–772.

Malik S, Guermah M, Yuan CX, Wu W, Yamamura S, Roeder RG. 2004. Structural and functional organization of TRAP220, the TRAP/mediator subunit that is targeted by nuclear receptors. *Mol Cell Biol* **24:** 8244–8254.

McKenna NJ, O'Malley BW. 2002. Combinatorial control of gene expression by nuclear receptors and coregulators. *Cell* **108:** 465–474.

Mishra A, Zhu XG, Ge K, Cheng SY. 2010. Adipogenesis is differentially impaired by thyroid hormone receptor mutant isoforms. *J Mol Endocrinol* **44:** 247–255.

Nishikata I, Sasaki H, Iga M, Tateno Y, Imayoshi S, Asou N, Nakamura T, Morishita K. 2003. A novel EVI1 gene family, MEL1, lacking a PR domain (MEL1S) is expressed mainly in t(1;3)(p36;q21)-positive AML and blocks G-CSF-induced myeloid differentiation. *Blood* **102:** 3323–3332.

Ohno H, Shinoda K, Ohyama K, Sharp LZ, Kajimura S. 2013. EHMT1 controls brown adipose cell fate and thermogenesis through the PRDM16 complex. *Nature* **504:** 163–167.

Pinheiro I, Margueron R, Shukeir N, Eisold M, Fritzsch C, Richter FM, Mittler G, Genoud C, Goyama S, Kurokawa M, et al. 2012. Prdm3 and Prdm16 are H3K9me1 methyltransferases required for mammalian heterochromatin integrity. *Cell* **150:** 948–960.

Puigserver P, Wu Z, Park CW, Graves R, Wright M, Spiegelman BM. 1998. A cold-inducible coactivator of nuclear receptors linked to adaptive thermogenesis. *Cell* **92:** 829–839.

Puigserver P, Adelmant G, Wu Z, Fan M, Xu J, O'Malley B, Spiegelman BM. 1999. Activation of PPARγ coactivator-1 through transcription factor docking. *Science* **286:** 1368–1371.

Roeder RG. 2003. Lasker Basic Medical Research Award. The eukaryotic transcriptional machinery: complexities and mechanisms unforeseen. *Nat Med* **9:** 1239–1244.

Rosen ED, Spiegelman BM. 2001. PPARγ: a nuclear regulator of metabolism, differentiation, and cell growth. *J Biol Chem* **276:** 37731–37734.

Rosen ED, Spiegelman BM. 2006. Adipocytes as regulators of energy balance and glucose homeostasis. *Nature* **444:** 847–853.

Rosen ED, Hsu CH, Wang X, Sakai S, Freeman MW, Gonzalez FJ, Spiegelman BM. 2002. C/EBPα induces adipogenesis through PPARγ: a unified pathway. *Genes Dev* **16:** 22–26.

Seale P, Kajimura S, Yang W, Chin S, Rohas LM, Uldry M, Tavernier G, Langin D, Spiegelman BM. 2007. Transcriptional control of brown fat determination by PRDM16. *Cell Metab* **6:** 38–54.

Seale P, Bjork B, Yang W, Kajimura S, Chin S, Kuang S, Scime A, Devarakonda S, Conroe HM, Erdjument-Bromage H, et al. 2008. PRDM16 controls a brown fat/skeletal muscle switch. *Nature* **454:** 961–967.

Seale P, Conroe HM, Estall J, Kajimura S, Frontini A, Ishibashi J, Cohen P, Cinti S, Spiegelman BM. 2011. Prdm16 determines the thermogenic program of subcutaneous white adipose tissue in mice. *J Clin Invest* **121:** 96–105.

Sears IB, MacGinnitie MA, Kovacs LG, Graves RA. 1996. Differentiation-dependent expression of the brown adipocyte

uncoupling protein gene: regulation by peroxisome proliferator-activated receptor γ. *Mol Cell Biol* **16:** 3410–3419.

Uldry M, Yang W, St-Pierre J, Lin J, Seale P, Spiegelman BM. 2006. Complementary action of the PGC-1 coactivators in mitochondrial biogenesis and brown fat differentiation. *Cell Metab* **3:** 333–341.

Wallberg AE, Yamamura S, Malik S, Spiegelman BM, Roeder RG. 2003. Coordination of p300-mediated chromatin remodeling and TRAP/mediator function through coactivator PGC-1α. *Mol Cell* **12:** 1137–1149.

Wu J, Bostrom P, Sparks LM, Ye L, Choi JH, Giang AH, Khandekar M, Virtanen KA, Nuutila P, Schaart G, et al. 2012. Beige adipocytes are a distinct type of thermogenic fat cell in mouse and human. *Cell* **150:** 366–376.

Wu J, Cohen P, Spiegelman BM. 2013. Adaptive thermogenesis in adipocytes: is beige the new brown? *Genes Dev* **27:** 234–250.